Water-Mediated Substrate/Product Discrimination: The Product Complex of Thymidylate Synthase at 1.83 Å[†,‡]

Eric B. Fauman, Earl E. Rutenber, Gladys F. Maley,[§] Frank Maley,[§] and Robert M. Stroud*

Department of Biochemistry and Biophysics, University of California, San Francisco, San Francisco, California 94143-0448

Received October 22, 1993[⊗]

ABSTRACT: In an irreversible enzyme-catalyzed reaction, strong binding of the products would lead to substantial product inhibition. The X-ray crystal structure of the product complex of thymidylate synthase (1.83-Å resolution, *R* factor = 0.183 for all data between 7.0 and 1.83 Å) identifies a bound water molecule that serves to disfavor binding of the product nucleotide, dTMP. This water molecule is hydrogen bonded to absolutely conserved Tyr 146 (using the *Lactobacillus casei* numbering system) and is displaced by the C7 methyl group of the reaction product thymidylate. The relation between this observation and kinetic and thermodynamic values is discussed. The structure reveals a carbamate modified N-terminus that binds in a highly conserved site, replaced by side chains that can exploit the same site in other TS sequences. The enzyme–products complex is compared to the previously determined structure of enzyme–substrate–cofactor analog. This comparison reveals changes that occur between the first covalent complex formed between enzyme and substrate with an inhibitory cofactor analog and the completed reaction. The almost identical arrangement of ligands in these two structures contributes to our model for the TS reaction and verifies the physiological relevance of the mode in which potent inhibitors bind to this target for rational drug design.

Thymidylate synthase (TS)[1] (EC 2.1.1.45) catalyzes the reductive methylation of deoxyuridylate (dUMP) to generate thymidylate (dTMP) in the sole *de novo* pathway for this DNA precursor (Stroud & Finer-Moore., 1993) (Figure 1). TS is a dimeric protein of identical monomers that uses methylenetetrahydrofolate (CH_2-H_4folate) both as the one-carbon source and as the reductant, converting it to dihydrofolate (H_2folate). Because of the increased need for thymidylate for DNA synthesis in rapidly dividing cells, TS is a focus of attention for inhibitor designs aimed at becoming anticancer drugs.

We have analyzed the structure of TS to understand on an atomic level the kinetics and catalysis (Finer-Moore et al., 1990; Stroud & Finer-Moore 1993) and to develop a method for the rational design and improvement of novel inhibitors (Shoichet et al., 1993). X-ray crystal structures of TS representing five key points along the reaction pathway have been described. These include the free enzyme from *Lactobacillus casei* (Hardy et al., 1987), from *Escherichia coli* (Perry et al., 1990), and from human TS (Schiffer et al., 1991), with substrate dUMP bound (Finer-Moore et al., 1993), with just cofactor bound (Kamb et al., 1992b), a ternary complex in which dUMP is covalently bound to C198(146) and a cofactor analog that is a potent noncovalent inhibitor of TS, CB3717 (Figure 1) (Montfort et al., 1990a; Matthews et al., 1990a), and with a polyglutamylated CB3717 (Kamb et al., 1992a), a ternary complex that resembles the covalent addition of cofactor to substrate with FdUMP and CH_2-H_4folate bound (Matthews et al., 1990b). TS undergoes a large conformational change upon binding both dUMP and folate analogs (Montfort et al., 1990a,b). Various secondary structural elements move toward the active site in a motion we term segmental accommodation which serves to sequester

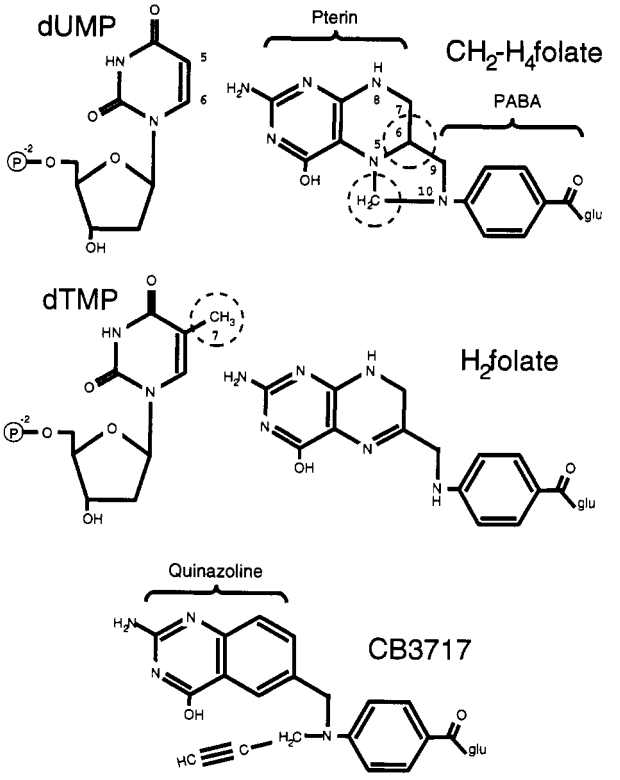

FIGURE 1: Chemical structures of TS ligands. Positions in the structures mentioned in the text are indicated, as are named fragments of the folates and folate–analog. The source and destination of the methylene and hydride are highlighted with dashed circles.

[†]This research was supported primarily by NIH Grants RO1-CA-41323 to J. F.-M. and R.M.S. and GM24485 to R.M.S., by NSF Grant DMB90-03737 to G.F.M. and Grant CA44355 to F.M. from the National Cancer Institute. E.B.F. received a Howard Hughes predoctoral fellowship. E.E.R. is an American Cancer Society postdoctoral fellow.

[‡]Coordinates for this structure have been submitted to the Brookhaven Protein Data Bank. The accession code is 1TYS.

* To whom correspondence should be addressed.

[§] Address: Wadsworth Center for Laboratories and Research, New York State Department of Health, Albany, NY 12201-0509.

[⊗] Abstract published in *Advance ACS Abstracts,* January 1, 1994.

[1] Abbreviations: TS, thymidylate synthase; ECTS, *E. coli* TS; dUMP, 2′-deoxyuridine 5′-monophosphate; dTMP, thymidine 5′-monophosphate; H_2folate, dihydrofolate; CH_2-H_4folate, 5,10-methylenetetrahydrofolate; CB3717, 10-propargyl-5,8-dideazafolate; rmsd, root mean square deviation.

0006-2960/94/0433-1502$04.50/0

the reactants away from bulk solvent. Our crystal structures show that dUMP alone binds in the open conformation, while binding of cofactor analog alone induces the transition to the closed form (Kamb et al., 1992b). Thus it is the binding of folate that leads to closure of the enzyme.

When the ECTS·dUMP·CB3717 complex was determined, it was noted that under nonreducing conditions the fused ring quinazoline portion of CB3717 occupied an alternate, well-defined binding pocket close to the functional site. The high degree of conservation of the residues in this large, sequestered alternate site suggested a functional role for this pocket, such as initial binding of the pterin ring of CH_2-H_4folate or postcatalytic binding of the reaction product H_2folate, so possibly participating in a mechanism for binding of reactants or release of products. In H_2folate the five-membered imidizolidine ring is opened, thus the structure of the product complex may test the notion that there may be a second site for transitional binding of CH_2-H_4folate that is occupied prior to release of dTMP.

The nucleotide product of the reaction, dTMP, differs from the substrate, dUMP, by a single methyl group at the C-5 position. However, dTMP binds 3–7-fold less tightly (Galivan et al., 1976; Beaudette et al., 1980; Santi & Danenberg, 1984), which may be important for product release. Because the reaction involves first transfer of methylene and then a hydride transfer step, the reaction is essentially irreversible. Thus, any degree of product binding contributes to product inhibition.

To understand the molecular basis of discrimination between nucleotides, to discern the binding mode of H_2folate, and to learn the conformational state of the enzyme upon completion of the chemistry of bond rearrangements, we determined the structure of the enzyme bound to the reaction products, H_2-folate and dTMP. This ECTS·dTMP·H_2folate product complex is the first X-ray crystal structure to reveal the state of the enzyme after bond rearrangements.

Since some of the intermediates needed to define the changes in structure and orientation along the reaction pathway involve the substrate molecules, we used a mutant of TS with the active site cysteine replaced by a serine to minimize turnover. In this case, with the product complex this may not be an issue since the backward reaction, formation of dUM^{32}P from highly labeled dTM^{32}P (>3000 Ci/mmol), in the presence of H_2-folate could not be detected with wild-type TS. However, to simplify comparisons among some of the earlier intermediate structures in the reaction, we use C198(146)S for crystal structures of complexes of TS with the naturally occurring ligands, and here with the reaction products. The activity of the *E. coli* C198(146)S[2] variant is about 1000-fold less than wild type by spectrophotometric analysis (unpublished results) and about 5000-fold less by tritium release (Dev et al., 1988). Both C146S in *E. coli* and the analogous mutant (C198S) in *L. casei* TS fail to complement a TS deficient strain of *E. coli*, χ_{2913} (Climie et al., 1990), implying that it has very low activity; although k_{cat} is greatly affected, the dissociation constant for dUMP is relatively unchanged (Dev et al., 1988).

MATERIALS AND METHODS

Protein and Crystals. The *E. coli thyA* gene in M13mp9 was mutated to C198(146)S using the method of Taylor et al. (1985) and then transferred as a *Hind*III fragment to pUC19 that was transformed into *E. coli* χ_{2913} (DthyA572). After induction to 5–10% of the cellular protein, the mutated enzyme was purified as described (Maley & Maley, 1988). Ternary complex crystals were grown by hanging drop cocrystallization of TS C198(146)S with the reaction products dTMP and H_2folate. A 5.0-μL drop of protein solution [20 mM KPO_4 pH 8.0, 1.5 mg/mL TS C198(146)S, 1.9 mM H_2folate, 5.8 mM dTMP, 3.8 mM $MgCl_2$, 3.8 mM dithiothreitol (DTT), 0.05 mM disodium ethylenediaminetetraacetic acid (EDTA), and 1.25 M $(NH_4)_2SO_4$] was equilibrated at 23 °C against an excess of precipitant solution [2.5 M $(NH_4)_2SO_4$ and 20 mM KPO_4, pH 8.0]. Golden, highly birefringent crystals with hexagonal bipyramidal morphology (250 μm × 250 μm × 450 μm) grew in 2–3 days. The cell dimensions are $a = b = 71.97$ Å, $c = 115.04$ Å, $\alpha = \beta = 90°$, and $\gamma = 120°$. Systematic absences along c^* such that $l = 3n$ only narrowed the choice of space groups to $P3_121$ or $P3_221$. Diffraction intensities were collected at the Stanford Synchrotron Radiation Laboratory on Port 7-1 using a MAR imaging plate, 1.09-Å radiation, 2° frames, and data collection times of 15–30 s. Two crystals cooled to 4 °C each yielded complete data sets, for a total of 228 243 independent observations to a resolution of 1.83 Å with observable diffraction extending beyond 1.5 Å. Intensities were integrated using the program DENZO (Otwinowski, 1986). Observations were scaled and reduced in point group 321 using the method of Fox and Holmes (1966) to give 30 830 unique reflections with an overall *R*sym[3] for intensities of 9.4%. Amplitudes were assigned to weak and negative intensities by fitting to an *a priori* distribution (Wilson, 1949; French & Wilson, 1978).

Structure Solution. The structure was solved by molecular replacement using the first monomer of the reported ECTS·dUMP·CB3717 ternary complex (Montfort et al., 1990a), with the ligands and water molecules omitted, as a search model. A rotation search followed by rigid body refinement was carried out using Patterson correlation, implemented using the approach of Brünger (1990). Of the top 106 coalesced peaks generated using amplitudes with $F/\sigma_F > 2.0$ between 15.0- and 4.0-Å resolution and Patterson space vectors between 30 and 5 Å, the top solution had a Patterson correlation coefficient of 0.105 . This solution was consistent with a monomer in the asymmetric unit, where the physiological dimer would be generated by the crystallographic 2-fold along $(x,x,0)$. This monomer was rotated by 120° about **c** so that a one-dimensional translation search could be conducted in the [1,0,0] direction. A translation search in $P3_121$ along $(x,0,{}^1/_3)$ using amplitudes with $F/\sigma_F > 2.0$ between 8.0 and 3.5 Å resolution gave a solution with an *R* factor[4] of 42%. A search in $P3_221$ along $(x,0,{}^1/_6)$ with the same data gave a top solution with an *R* factor of 51%. The transformed coordinates were refined in $P3_121$ by rigid body least-squares minimization

[2] Numbering of residues is by the *L. casei* convention, as in Hardy et al. (1987). *E. coli* sequence numbers are given in parentheses after the *L. casei* numbering throughout the text.

[3]
$$R_{sym} = \frac{\sum_{hkl}\sum_{i=1}^{N}(I_{avg} - I_i)^2}{\sum_{hkl}\sum_{i=1}^{N}(I_i)^2}$$

[4]
$$R = \frac{\sum_{hkl}|(|F_o| - |F_c|)|}{\sum_{hkl}|F_o|}$$

Table 1: Crystallographic Data Statistics

resolution (Å)	∞–5.60	4.00	3.27	2.84	2.54	2.32	2.15	2.01	1.90	1.80
R_{sym} (I) (%)	5.6	5.5	6.7	8.6	11.3	14.3	17.3	21.6	27.5	38.3
av I/sig(I)	8.8	8.9	8.5	6.7	5.3	4.3	3.6	3.0	2.4	1.7
unique reflections possible	1254	1999	2544	2927	3352	3634	3898	4294	4274	4845
unique reflections collected	1117	1942	2506	2889	3313	3597	3860	4254	4235	3117
completeness of data (%)	89	97	99	99	99	99	99	99	99	64
redundancy	7.3	8.0	8.0	8.0	7.7	7.6	7.5	7.1	7.0	6.1
resolution bins for R factor (Å)		7.0–3.59	2.92	2.57	2.34	2.18	2.05	1.95	1.87	1.80
R_{cryst} of refined structure (%)		13.6	15.6	18.2	19.6	20.4	23.0	24.6	28.2	31.2

Table 2: Structural Statistics

RMS deviationsfrom idealityin final model[a]	bond lengths (Å)	bond angles (deg)	dihedral angles (deg)	improper angles (deg)[b]	Ponder-Richards (%)[c]	Ramachandran outliers[d]
ECTS·dTMP·H_2folate	0.012	2.68	25.08	1.01	95	0
ECTS·dUMP·CB3717	0.010	2.78	25.68	1.23	94	3
Montfort et al. (1990a)[e]	0.030	5.07	28.52	3.81	85	3

[a] Measured for all non-hydrogen atoms against X-PLOR target values. [b] Improper angles define chiral centers and planar groups of atoms. [c] Percent of residues which can be assigned to one of the rotamers identified by Ponder and Richards within 3 standard deviations. [d] Number of non-glycine residues that fall outside allowed regions for left-handed helix, β-strand, α-helix, or the "saddle" region between β-strand and α-helix. [e] Previously reported ECTS·dUMP·CB3717 structure, which was refined against PROLSQ target values.

using X-PLOR to give an R factor of 36.7% using all data between 15.0 and 4.0 Å.

A difference electron density map [$(F_o - F_c)\ \alpha_c$] calculated using the rigid-body refined model displayed clear, detailed density for the ligands H_2folate and dTMP, including distinct density for the C7 methyl group of dTMP, confirming that the rotation and translation solutions were correct. The ligands were modeled into the difference electron density using FRODO (Jones, 1985). The complete model was subjected to alternating cycles of positional and B factor refinement, including one round of simulated annealing (Brünger, 1989) and hand rebuilding. As a final step, occupancies and B factors for the water molecules only were refined in alternating cycles. The final R factor is 18.3% for all data between 7.0 and 1.83 Å for a model with a total of 2386 atoms, including 164 water molecules. Two residues, Met 10(8) and Leu 260(208) are modeled with two alternate conformations.

The ECTS·dUMP·CB3717 structure, refined to 1.97 Å (Montfort et al., 1990a), was previously the highest resolution TS structure reported. That structure had been refined using PROLSQ (Hendrickson & Konnert, 1979). To facilitate comparison between the ECTS·dUMP·CB3717 and the ECTS·dTMP·H_2folate complexes and to distinguish differences due to the increased resolution, different space group, different refinement schemes, and different ligands, the ECTS·dTMP·H_2folate complex coordinates were used to initiate further refinement of the ECTS·dUMP·CB3717 structure. A dimer of the ECTS·dTMP·H_2folate coordinates was rotated into the $P6_3$ space group, dUMP and CB3717 were placed in the active sites, and the waters from ECTS·dTMP·H_2folate were retained. These coordinates were subjected to simulated annealing refinement to minimize the bias from the starting structure. This was followed by alternating cycles of hand-rebuilding and refinement through minimization. This new refined ECTS·dUMP·CB3717 structure was used for all further structural comparisons.

ECTS·dTMP·H_2folate was superimposed on ECTS·dUMP·CB3717 by selecting a core of Cα atoms in the dimer according to the congruence of difference distance matrices (Perry et al., 1990) and orienting to minimize the rms deviation between these Cα positions in the two structures (Kabsch, 1978), using the programs NEWDOME and GEM (Fauman, 1993).

RESULTS

Analysis of the Structure. The product complex is the highest resolution for TS and lies in a different space group than the large number of independently refined TS structures, which include four solved using independent heavy atom solutions (Hardy et al., 1987; Montfort et al., 1990a; Matthews et al., 1990a,b). There are no ambiguities in the main chain. The high quality of this structure is reflected in the final R factor of 0.18- to 1.83-Å resolution, detailed in the crystallographic statistics (Table 1), by the level of constraints, with no residues that fall outside the optimal regions of the Ramachandran plot of ϕ and ψ angles (Table 2), and seen in the electron density map (Figures 2 and 3). A $2F_o - F_c$ electron density map contoured at a 1σ level displays continuous density for all but parts of a few surface side chains. The electron density for most aromatic groups displays a hole through the center of the ring, characteristic of high-resolution structures. Within 3 standard deviations 95% of the side chains are matched to the rotamers identified by Ponder and Richards (1987).

New Packing Arrangement. E. coli TS is a dimer of identical 30-kD monomers. The trigonal space group $P3_121$, observed for ECTS·dTMP·H_2folate but previously unreported for an ECTS crystal, places a single monomer in the asymmetric unit. Crystal structures of the phosphate- and nucleotide-bound binary complexes of the enzyme (Hardy et al., 1987; Perry et al., 1990; Schiffer et al., 1991; Finer-Moore et al., 1993) also have a monomer in the asymmetric unit. Our previously reported structures for ternary complexes of TS (Montfort et al., 1990a; Kamb et al., 1992a) and folate-bound (Kamb et al., 1992b) crystal structures, however, have crystallized in space group $P6_3$, with a dimer in the asymmetric unit. Under the crystallization conditions described here, the presence of both dTMP and H_2folate are required to yield crystals in space group $P3_121$, since crystallization with either one of these ligands alone did not result in this space group.

In the ECTS·dUMP·CB3717 structure, which lies in space group $P6_3$, the lattice contacts are different between the two monomers in the asymmetric unit (Figure 4). In ECTS·dTMP·H_2folate, there is a single monomer in the asymmetric unit, and the crystal contacts are the same to both monomers of the physiological dimer. These contacts are different from those observed for either of the monomers in the ECTS·

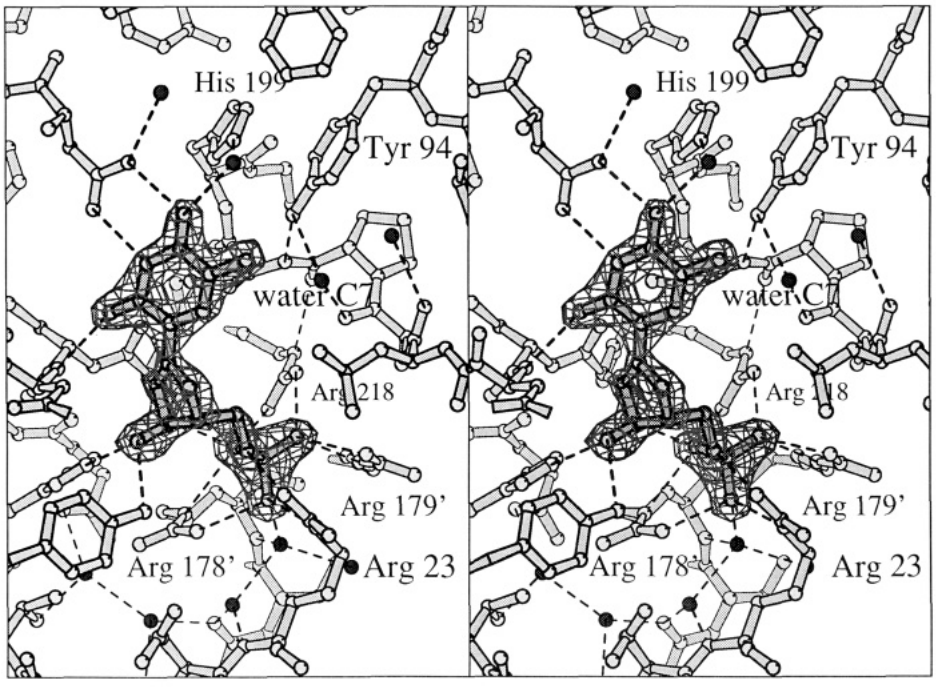

FIGURE 2: Cross-eyed stereoview of dTMP binding. The nucleotide ligand is clearly revealed in this $F_o - F_c$ electron density omit map, contoured at 6σ. Before calculating this map, both ligands were removed from the F_c calculations. The C7 methyl group can be seen on the right side of the pyrimidine ring. Residues mentioned in the text are labeled. Selected hydrogen bonds (<3.1 Å) are indicated with dashed lines. Crystallographic waters are depicted as dark circles.

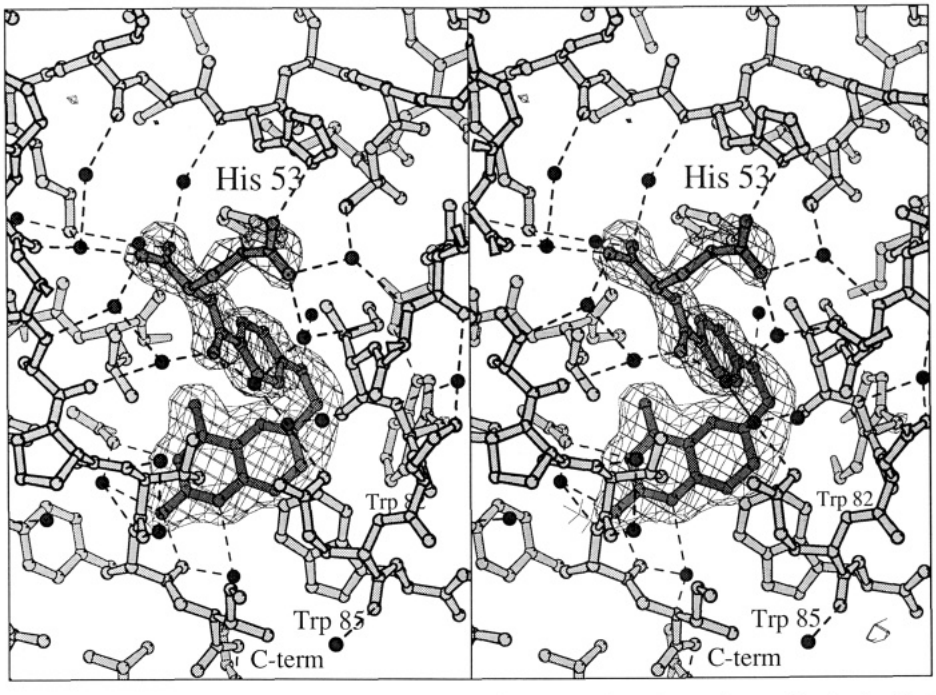

FIGURE 3: Cross-eyed stereoview of H_2folate binding. All atoms of the folate ligand are in continuous density in this $F_o - F_c$ electron density omit map, contoured at 3σ. Before calculating this map, both ligands were removed from the F_c calculations. Residues mentioned in the text are labeled. Selected hydrogen bonds (<3.1 Å) are indicated with dashed lines. Crystallographic waters are drawn as dark circles.

dUMP·CB3717 structure, though they are more similar to the lattice contacts for the second monomer (Figure 4).

The number of crystal contacts, defined as symmetry-related atoms located less than 3.5 Å away, is the same in both the $P3_121$ and the $P6_3$ crystal forms. However, the number of hydrogen bonds closer than 3.2 Å between dimers is higher in the $P3_121$ crystals, with 24 hydrogen bonds/dimer, as compared to only 14 hydrogen bonds/dimer in the $P6_3$ crystal form. Since the packing density is roughly the same in both space groups, 54% solvent in the $P3_121$ crystal form vs 51% in the $P6_3$ crystal form, these extra hydrogen bonds may contribute to the improved resolution of the data obtained from the ECTS·dTMP·H_2folate crystals. The most extensive crystal contacts in ECTS·dTMP·H_2folate occur at residues His 53(51) and Arg 55(53), concurrent with large shifts in position for these residues compared to ECTS·dUMP·CB3717 (Figure 4).

Structure Comparison. In order to determine which differences in structure observed between the ECTS·dUMP·CB3717 and the ECTS·dTMP·H_2folate complexes are due simply to the improved resolution of the current structure,

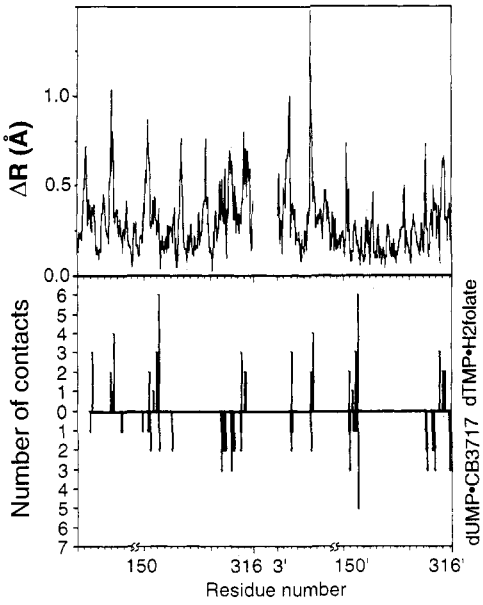

FIGURE 4: Changes in structure compared to crystal contacts. The top half of the figure plots the difference Δr in Cα position between ECTS·dUMP·CB3717 and ECTS·dTMP·H_2folate after superimposition of the dimers. The first monomer contains residues 3–316, the second 3–316. The lower half of the figure shows the number of different atom–atom contacts less than 3.5 Å. Contacts in ECTS·dUMP·CB3717 are indicated below the line, while those in ECTS·dTMP·H_2folate are above the line.

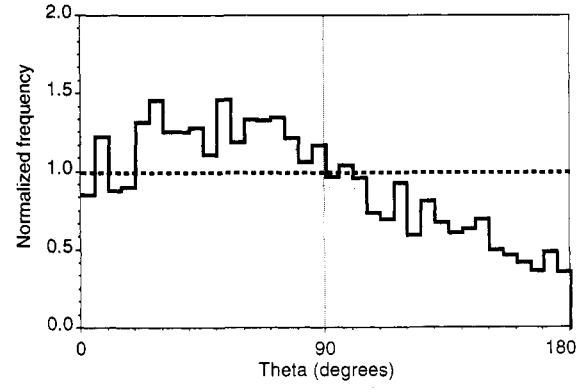

FIGURE 5: Shrinkage. Although the atomic shifts between ECTS·dUMP·CB3717 and ECTS·dTMP·H_2folate are very small, the inward bias of the direction of the shifts is revealed in this histogram. Theta is the angle between the vector from the atom to the center of mass for the dimer and the shift direction for that atom. Thus, a movement straight toward the center of mass would be an angle of 0°. The values are binned in 5° intervals and plotted as the number of occurrences in each bin, divided by the number expected based on random motion, which, for a bin from θ_1 to θ_2, is $[\cos\theta_1 - \cos\theta_2]/2(\theta_2 - \theta_1)$. The straight line at frequency = 1.0 indicates the graph expected if there were no bias. The dimer, and also each monomer considered separately (not shown), all show a greater shifts toward the center ($\theta < 90°$) than away ($\theta > 90°$), indicating that the ECTS·dTMP·H_2-folate structure is closed down slightly more than the ECTS·dUMP·CB3717 structure.

ECTS·dUMP·CB3717 was rerefined starting with the ECTS·dTMP·H_2folate complex as a model. This newly refined structure has the same R factor as the previous structure, but improved geometry (Table 2). The Cα positions changed by only 0.19 Å rmsd. The largest change occurred between residues 155 and 156 where a flip of the peptide plane was discovered in both the ECTS·dUMP·CB3717 and the ECTS·dTMP·H_2folate complexes relative to the original reported ECTS·dUMP·CB3717 structure. Further, extra density was observed confluent with the Sγ of Cys 52(50) and Cys 244(192) in both monomers. This was modeled as a single additional sulfur and may reflect reaction of the protein with β-mercaptoethanol, the reducing agent that was added during crystal growth. The overall rmsd between the reported and the newly refined ECTS·dUMP·CB3717 structures is 0.73 Å for all atoms in the protein, mostly due to those few side chains assigned to new rotamers.

The protein in ECTS·dTMP·H_2folate is in the closed conformation, as induced by the binding of cofactor. After superimposition of the dimers, there is an rmsd of 0.35 Å in Cα position (0.66 Å for all atoms in the protein) between this and the ECTS·dUMP·CB3717 structure. Although the monomers are similar in both space groups, there is a change in the association of the monomers. In ECTS·dUMP·CB3717, the monomers are asymmetrically disposed, related by a rotation of 179.5° about an axis with direction cosines of (–0.0012, 0.4302, 0.9027) with respect to $P6_3$ orthogonalized axes and with a slight translation of 0.08 Å along the rotation axis. Thus, not only is the axis not a perfect 2-fold but it is far from where the 2-fold would have to be for the ECTS·dUMP·CB3717 structure to lie in a higher symmetry space group ($P6_322$). The monomers in ECTS·dTMP·H_2-folate are related by a strict crystallographic 2-fold rotation axis (parallel to the **a** axis).

Because of this change in association, the monomers of each structure superimpose better than the whole dimers. Monomer 1 of the ECTS·dUMP·CB3717 structure superimposes on the monomer in the ECTS·dTMP·H_2folate structure with a rmsd of 0.30 Å for Cαs (0.60 Å all atoms); monomer 2 superimposes with a rmsd of 0.29 Å for Cαs (0.66 Å all atoms). This is even smaller than the differences between the two monomers in ECTS·dUMP·CB3717, which have a rmsd of 0.33 Å for Cαs (0.75 Å all atoms).

Although the magnitude of the positional differences is very small, there is an inward bias to the shifts (Figure 5). Thus the product complex ECTS·dTMP·H_2folate is slightly more closed than ECTS·dUMP·CB3717. This is reflected in the radius of gyration for the dimer, which decreases from 23.12 Å for ECTS·dUMP·CB3717 to 23.04 Å in ECTS·dTMP·H_2-folate.

Ligand Binding. dTMP and H_2folate are well defined in the electron density maps (Figures 2 and 3). The positions of the ligands in the substrate-like ECTS·dUMP·CB3717 and product ECTS·dTMP·H_2folate complexes are almost identical. There is an rmsd of 0.27 Å for all matching atoms in the nucleotide and 1.11 Å for all matching atoms in the folate and CB3717. The ECTS·dUMP·CB3717 structure shows a covalent bond between the Sγ of Cys 198(146) and the C6 of the dUMP. The protein in ECTS·dTMP·H_2folate is a Cys to Ser variant, and there is no covalent bond present. Instead the serine side chain rotates from the gauche$^-$ rotamer (χ_1 = –52°) seen for Cys 198(146) in ECTS·dUMP·CB3717 to the trans rotamer (χ_1 = 151°) and establishes a hydrogen bond to the main chain carbonyl of Ser 219(167).

All noncovalent interactions around the ligands reported for ECTS·dUMP·CB3717 (Finer-Moore et al., 1990) are preserved in ECTS·dTMP·H_2folate, with the following exceptions: (a) The C-terminal carboxylic acid and Nϵ of Trp 85(83), hydrogen bonded in monomer 1 of the ECTS·dUMP·CB3717 complex, are 3.8 Å apart in ECTS·dTMP·H_2-folate. This hydrogen bond is also absent in monomer 2 of ECTS·dUMP·CB3717. (b) There are additional interactions between the phosphate moiety of the nucleotide and the quartet of arginine side chains that are coordinately bound to it (Table 3) so that now each arginine forms two distinct hydrogen bonds to the phosphate. (c) Phe 228(176), which

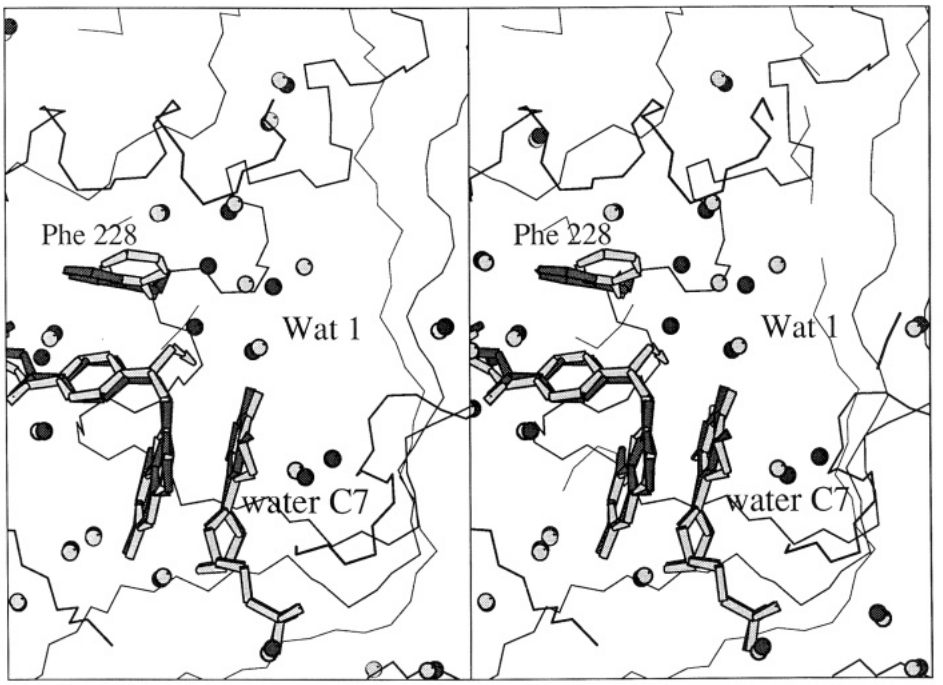

FIGURE 6: Cross-eyed stereoview of Phe 228(176) in ECTS·dTMP·H_2folate (black bonds) that moves away from the site of the propargyl group in ECTS·dUMP·CB3717 (white bonds). A water occupies the site of the propargyl, and two waters near the phenylalanine move in concert with the side chain. Most other waters have identical positions in both ternary complex structures, with the notable exception of water^{C7}, to the right of the nucleotide.

Table 3: Hydrogen Bonds to the Phosphate in ECTS·dTMP·H_2folate

arginine atom	phosphate atom	distance (Å)[a]	angle (deg)[b]
Nε 21	OP1	2.82	161
Nη1 21	OR5	3.01	169
Nη1 166	OP3	2.73	152
Nη2 166	OP2	2.80	151
Nε 126	OP2	3.05	135
Nη1 126	OP1	3.01	163
Nε 127	OP3	2.84	142
Nη1 127	OP3	2.79	144

[a] Distance between the named atoms. [b] Optimal donor–hydrogen–acceptor angle, assuming a donor–hydrogen bond length of 1.0 Å and that the phosphate is the hydrogen bond acceptor in all cases.

interacts with the PABA moiety of the folate, has shifted, with a change in χ_2 angle from −150° to −85°, moving away from the propargyl group of CB3717. The shift in the side chain repositions two waters. An additional water takes the place of the propargyl group of CB3717 (Figure 6).

Thymidylate differs from deoxyuridylate by the presence of a methyl group, C7, at the C5 position in the pyrimidine ring. In ECTS·dTMP·H_2folate, the only residue that comes within 3.5 Å of this methyl group is the side chain of the absolutely conserved Trp 82(80), which also interacts with the pterin of the folate. This residue is virtually unperturbed, rotating only 3° between ECTS·dUMP·CB3717 and ECTS·dTMP·H_2folate.

A water molecule, water^{C7}, is shifted 0.5 Å away from the ligands to a position 3.4 Å from the C7 methyl (Figures 2 and 6). This water is coordinated by the carbonyl of Ala (196)144 and the side chain hydroxyl of absolutely conserved Tyr 146(94), which in turn is also hydrogen bonded to the main chain nitrogen of Ser 198(146). More dramatic than the shift in position is the decrease in occupancy of water^{C7}. In the ECTS·dUMP·CB3717 structure, water^{C7} has full occupancy and a *B* factor of 9 Å^2, close to the average of 9 Å^2 for the ligating atoms. However, in the product complex ECTS·dTMP·H_2folate, the relative occupancy of water^{C7} is reduced to only 0.5, and the *B* factor increased to 16 Å^2, close to the average of 16 Å^2 for the ligating atoms. In addition, there is another, or better ordered, water molecule, not sufficiently occupied to be assigned in the ECTS·dUMP·CB3717 structure, located 3.3 Å farther removed from methyl C7 which has a relative occupancy of 0.3 and a *B* factor of 20 Å^2. This partial water is shown to the right of water^{C7} and hydrogen bonded to the carbonyl of Leu 195(143) in Figure 2.

Function of the Modified N-Terminus. Improved resolution reveals some novel features in the thymidylate synthase structure. One is the presence of a chemical modification at the N-terminal amino group, which consists of three covalently attached atoms (Figure 7). This modification is also present in the ECTS·dUMP·CB3717 structure. These atoms are coplanar with the main chain nitrogen; the two terminal atoms are hydrogen bonded to the side chains and main chain of highly conserved Thr 48(46) and Thr 49(47). [Thr 49(47) is a leucine in *Lactobacillus lactis* TS (Ross et al., 1990).]

Since both terminal atoms receive hydrogen bonds from main chain N–H groups (Table 4), these atoms are identified as oxygens, implying a carbamate involving the N-terminal nitrogen. The two terminal oxygens have full occupancy and *B* factors of 17 and 18 Å^2, close to that for the backbone atoms of residue Met 3(1) (19 Å^2); thus the modification is not simply a formyl group. In solution, carbamic acids rapidly decompose to release free carbon dioxide. In the context of the protein it appears that the carbamate is stabilized by the threonine pocket, where it is sheltered from bulk solvent.

To test the roles of Thr 48(46), and Thr 49(47), these residues were mutated to valine in *E.coli* TS. Thr 49(47)Val TS had a k_{cat} of 52.4 min^{-1}, about 10% wild-type activity (k_{cat} = 410 min^{-1}) based on turnover under saturating conditions of both substrates at 30 °C. When both variants were introduced together, Thr 49(47), Thr 48(46)Val TS has zero activity. Thus both of the carbamate-binding residues are clearly important in generating the functional catalytic site, presumably involving the modified N-terminus.

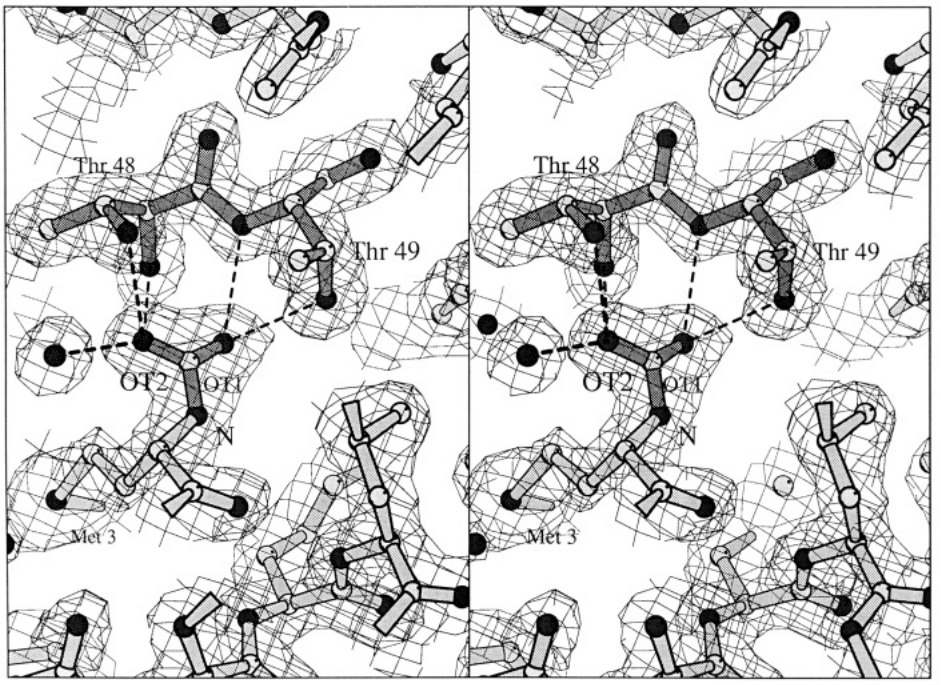

FIGURE 7: Cross-eyed stereoview of the N-terminal modification. The clear continuous density for the N-terminal modification is visible in this $2F_o - F_c$ electron density map, contoured at 1σ. Carbons are displayed as light circles while non-carbons are drawn as dark circles. Hydrogen bonds involving the N-terminal modification are indicated by dashed lines.

Table 4: Hydrogen Bonds to the N-Terminal Modification

atom1	atom2	distance (Å)[a]	angle (deg)[b]
OT1	Thr[49] Oγ1	2.78	175
OT1	Thr[49] N	2.98	155
OT2	Thr[48] Oγ1	2.72	176
OT2	Thr[48] N	3.00	156
OT2	Wat[574]	2.79	180

[a] Distance between the named atoms. [b] Optimal donor–hydrogen–acceptor angle, assuming a donor–hydrogen bond length of 1.0 Å and that the carbamate is the hydrogen bond acceptor in all cases.

Table 5: Reported Dissociation Constants for dUMP and dTMP

method	K_d dUMP (μM)	K_d dTMP (μM)	K_d dTMP/K_d dUMP
equilibrium dialysis[a]	1.80	5.75	3.2
equilibrium dialysis w/H_2folate[b]	0.52	3.27	6.3
kinetics[c]	0.32	2.37	7.4
thermal titration[d]	5.9	17.5	3.0
competition with PLP[e]	0.38	1.60	4.2

[a,b] Galivan et al. (1976). [c] Daron and Aull (1978). [d] Beaudette et al. (1980). [e] D. V. Santi (personal communication). PLP is pyridoxal, an inhibitor of TS.

DISCUSSION

Selectivity in Nucleotide Binding. The pyrimidine nucleotides dUMP and dTMP differ by the replacement of hydrogen by a methyl group at the C5 position in dTMP. However, dUMP is bound 3–7 times more tightly than dTMP, either with or without cofactor in studies on TS from *L. casei* (Table 5). By thermal titration, Beaudette (1980) showed that dUMP binding is driven primarily by enthalpy change (ΔG = –7.1 kcal/mol, ΔH = –5.4 kcal/mol, $-T\Delta S$ = –1.7 kcal/mol). Thymidylate binding, however, is purely entropy driven (ΔG = –6.7 kcal/mol, ΔH = 0.7 kcal/mol, $-T\Delta S$ = –7.4 kcal/mol). This is consistent with the observation that dTMP is more hydrophobic than dUMP, as measured by partition coefficients from water to octanol (Hansch & Leo, 1979), since hydrophobically driven associations are usually accompanied by an increase in entropy and a small decrease in enthalpy (Dill et al., 1989; Da et al., 1992).

The added hydrophobicity of the C7 methyl group is illustrated dramatically at the atomic level by the perturbation of water^{C7} near the C7 of dTMP (Figures 2 and 6). Water^{C7} is coordinated by the hydroxyl oxygen of absolutely conserved Tyr 146(94) and the main chain carbonyl of Ala 196(144). The presence of the methyl group shifts the water molecule and greatly decreases its occupancy at this site. Thus, it appears that, in addition to the solution phase entropic and enthalpic perturbations of the C7 methyl group, the enzyme is able to discriminate between the substrate and product nucleotides through this water molecule. In the absence of the C7 methyl group, water^{C7} is present and makes two strong hydrogen bonds to the protein. With the C7 methyl, this water is displaced, costing in enthalpy through the loss of hydrogen bonds to the two protein atoms but gaining in entropy through the disordering of a bound water molecule.

The removal of a bound water molecule is thermodynamically analogous to a water molecule in the melting of ice which is accompanied by a gain in entropy but a loss in enthalpy. This was illustrated by Vriend et al. (1991) in an experiment in which an alanine was replaced by serine in the neutral protease of *Bacillus stearothermophilus*. The serine displaced a bound water molecule and replaced the hydrogen-bonding interactions. This results in a more stable protein, since the water is released to bulk solvent and there is no net loss of hydrogen bonds within the protein. In TS, however, the hydrogen bonds to water^{C7} are not compensated for in the protein, and a small cavity is left behind, which is also energetically unfavorable (Rashin et al., 1986). Thus, in the case of TS, the waterless state (ECTS·dTMP) is less stable than the water-bound state (ECTS·dUMP).

Water-mediated ligand selectivity is also exhibited by the L-arabinose-binding protein. Through crystallographic analysis, Quiocho et al. (1989) showed that bound waters are responsible for favorable interactions to hydroxyl groups in L-arabinose and D-galactose (which bind with K_d values of 98

and 230 nM, respectively) and unfavorable interactions with a methyl group in D-fucose (which has a K_d of 3.8 mM). In TS, the water^{C7} makes no favorable interactions to either ligand, and correspondingly the degree of selectivity is less in TS than in the L-arabinose-binding protein.

Aside from its role in ligand binding, water^{C7} may be involved in the chemistry of TS. A key step in the reaction involves the removal of the proton from C5 (Pogolotti & Santi, 1977; Finer-Moore et al., 1990; Matthews et al., 1990b; Stroud & Finer-Moore, 1993). However, no amino acid side chains are positioned to fulfill this role directly. Water^{C7}, 4 Å away, is the closest nonligand atom to C5 (other than the Sγ of Cys 198(146), covalently bonded to C6 of dUMP) in the ECTS·dUMP·CB3717 structure. It could act as the base and accept the proton from C5. At the proton-abstraction stage, C5 of dUMP is tetrahedral, with the C7 methylene covalently attached to the folate and directed away from the water^{C7} position; the C5 proton is directed away from the folate such that the C5–C5H proton vector would point almost directly at water^{C7}. Removal of the C5H hydrogen results in a planar C5, which brings the C7 methylene closer to the position seen in the ECTS·dTMP·H_2folate structure, displacing water^{C7}.

Another nearby water observed in the covalent complexes, Wat 1 in the ECTS·dUMP·CB3717 structure of Finer-Moore et al. (1990), Wat 401 in the ECTS·FdUMP·CH_2-H_4folate structure of Matthews et al. (1990b), is 4.5 Å from C5 and is hydrogen bonded to the O4 of dUMP, the absolutely conserved Glu 60(58), and the highly conserved His 199(147). This water serves to stabilize the enolate oxygen formed in the covalent Michael adduct. Wat 1 (Wat 401) was favored by Matthews et al. (1990b) as the possible hydrogen acceptor for the C5 proton. However, Wat 1 is on the same side of the pyrimidine ring as the folate and is not in as good a position to receive the proton (Figures 2 and 6). Mutagenesis of Tyr 146(94) and neighboring residues may elucidate the involvement of water^{C7} and Wat 1 further.

Predicted Mechanism of Hydroxymethylases. There is another possible chemical role for water^{C7}. In a reaction similar to that of TS, the pyrimidine hydroxymethylases transfer a methylene group from CH_2-H_4folate to the C5 position of a pyrimidine nucleotide. However, instead of hydride transfer from the cofactor, the hydroxymethylases add a hydroxyl to C7, resulting in a hydroxymethyl group. Sequences of two hydroxymethylases are known: a dCMP hydroxymethylase (Lamm et al., 1987; Thylen, 1988) that is 24% identical to ECTS and a dUMP hydroxymethylase (Wilhelm & Ruger, 1992) that is 22% identical to ECTS [aligned using the program GAP (Devereux et al., 1984)]. Tyr 146(94) is conserved in these enzymes, and therefore we expect water^{C7} to be present in a similar position. In ECTS·dTMP·H_2folate, water^{C7} is 3.4 Å from C7 and is nearly aligned with the π orbital, with an angle of 114° between C5 to C7 and C7 to water^{C7}, in a good position to add to a C7 methylene (optimum 90°). However, the C6 of the pterin moiety, the source of hydride transfer in the TS reaction (Lorenson et al., 1967), remains exquisitely positioned in the active site of the product complex, to have been available for hydride transfer to the C7 methylene. It is 3.6 Å away from the C7 methyl group, making an angle of 85° with the C5 and C7 bond of dTMP. Thus, the C6 hydrogen of the pterin ring is better positioned in TS to donate to C7, resulting in the creation of a methyl group. In the hydroxymethylases the nearby water molecule may be better positioned and so be the source of the hydroxymethyl group at C7.

From structure and mutagenesis it is clear that the C-terminus is key to positioning of the folate cofactor (Perry et al., 1993). Deletion of just the last residue results in a protein that can bind both ligands but is catalytically inactive (Galivan et al., 1977; Carreras et al., 1992) because the protein is incapable of closure to sequester the reactants (Perry et al., 1993). Mutants of Val 316(264), the last residue in *L. casei* TS, have a higher K_m for the cofactor, while K_m for the nucleotide is little changed (Climie et al., 1992). Both hydroxymethylase sequences known, while preserving many key residues, differ greatly at the C-terminus. Deoxycytidylate hydroxymethylase terminates 40 amino acids before the TS C-terminus, while dUMP hydroxymethylase contains an extra 120 amino acids beyond the C-terminus of TS. As both sequences were isolated from bacteriophage, it is possible that the hydroxymethylases are simply TSs that have diverged to the point where methylene transfer can take place, but the folate C6H hydride donor is no longer perfectly aligned, allowing for hydroxyl transfer from water^{C7} to complete the reaction. A mechanism for dUMP hydroxymethylase consistent with these predictions has been proposed by Kunitani and Santi (1980).

Folate Binding and Overall Protein Conformation. The ECTS·dUMP·CB3717 and ECTS·dTMP·H_2folate structures are very similar, with an rms deviation of only 0.35 Å in Cα position. The slight shrinkage illustrated in Figure 5 may be due to either the greater number of strong crystal contacts in ECTS·dTMP·H_2folate, or the lower data-collection temperature employed in collecting the ECTS·dTMP·H_2folate complex data (4 °C compared to 22 °C for ECTS·dUMP·CB3717).

The ECTS·dUMP·CB3717 complex mimics the first covalent addition in the reaction, with a covalent bond between the Sγ of Cys 198(146) and the C6 of the dUMP as occurs in the Michael addition reaction. The product complex structure ECTS·dTMP·H_2folate reported here represents the end point after methyl transfer, but prior to dissociation of products. The high degree of overlap between the ligands in the two structures suggests that relatively little conformational change occurs during carbon transfer and reduction, as opposed to the extensive segmental accommodation that occurs upon ligand binding (Stroud & Finer Moore, 1993). Thus it is likely that CH_2-H_4folate and dUMP in the activated complex are bound in the same conformation observed for the ligands in these two crystal structures, as in the model of the activated complex (Finer-Moore et al., 1990).

The location of the H_2folate pterin ring in the primary binding site identified for the quinazoline of CB3717 and absence from the alternate site does not support the notion that the alternate site is used for binding of H_2folate. Although the function of the alternate site is still unknown, it is surprising that it retains so many conserved side chains in a cavity sequestered from solvent and clearly adequate for highly compatible binding of a nanomolar inhibitor CB3717. It may be involved in the enzyme mechanism, and mutagenesis will assess the role.

The largest chemical difference between CB3717 and H_2-folate is the presence of the triple-bond containing propargyl group at N10 of CB3717 (Figures 1 and 6), which is important for the tight binding of that inhibitor. In the ECTS·dUMP·CB3717 complex, the aromatic ring of Phe 228(176) stacks against the propargyl group. This specific interaction is lost in the ECTS·dTMP·H_2folate structure, where Phe 228-(176) is rotated away from the site where the propargyl group would be, to make more extensive van der Waals contacts

with the *p*-aminobenzoic acid moiety of H_2folate.

Role of N-Terminal Carbamate. Improved resolution reveals new features in ECTS·dTMP·H_2folate. Principal among these is the N-terminal modification. The N-terminus in TS has a variable number of residues prior to residue 3(1), to the extent of having an entire additional protein in the case of the bifunctional DHFR-TS enzymes (Beverley et al., 1986). However, all TS sequences either begin with a methionine at position 3(1) as in *E. coli* TS or have an acidic side chain at this position. In the *L. casei* TS crystal structure (Finer-Moore et al., 1993), Glu 3(1) accepts hydrogen bonds from the threonine pocket that is occupied by the carbamate in *E. coli*. Thus this could be a conserved feature of TSs, which serves as a link between regions involved in segmental accommodation, similar to conserved Tyr 6(4) which links the A helix to the J helix, and conserved His 264(212) which links the K helix to the C-terminal strand.

Although carbamates are unstable in solution, they have been observed in protein crystal structures (Arnone, 1974; Lundqvist & Schneider, 1991). In ribulose 1,5-bisphosphate carboxylase, a carbon dioxide molecule modifies a lysine within the active site. In hemoglobin, carbon dioxide is transported from the muscles back to the lungs by covalent addition to the N-terminus as carbamate.

Conclusion. The X-ray crystal structure of the product complex of thymidylate synthase suggests that the enzyme uses a bound water molecule to disfavor binding of the product nucleotide. This water molecule, named water^{C7} for its proximity to the C7 atom of dUMP, may also be involved in proton abstraction from C5 after transfer of the methylene group in the reaction mechanism. An analogous water in the hydroxymethylases may be the source of the hydroxyl group after the methylene is transferred from CH_2-H_4folate, in the similar transfer of a hydroxymethyl in the catalytic mechanism.

At 1.83-Å resolution, this structure, besides identifying a previously unreported N-terminal modification, allows better positioning of all residues in the structure. Our ongoing inhibitor-design efforts are enhanced by this improved structure. Although the positional differences between ECTS·dTMP·H_2folate and ECTS·dUMP·CB3717 are slight, configurations of many side chains have been adjusted. In the dimer, though the backbone is unchanged by refinement except for a single amide, 179 of 528 side chains have been refined to different rotamers. The importance of water in enzyme catalysis is only just beginning to be recognized. In TS, water molecules play key roles in catalysis, and in substrate/product discrimination. We propose a new mechanism for the hydroxymethylases based on the homologous TS structures.

ACKNOWLEDGMENT

We thank Janet Finer-Moore, Chris Carreras, and Brian Shoichet for many useful discussions and Partho Ghosh for assistance with synchrotron data. *E. coli* strain X2913 was kindly provided by Dan Santi. Figures 2, 3, 6, and 7 were generated using MolScript (Kraulis, 1991).

REFERENCES

Arnone, A. (1974) *Nature 247*, 143–145.

Beaudette, N. V., Langerman, N., & Kisliuk, R. L. (1980) *Arch. Biochem. Biophys. 200*, 410–417.

Beverley, S. M., Ellenberger, T. E., & Cordingley, J. S. (1986) *Proc. Natl. Acad. Sci. U.S.A. 83*, 2584–2588.

Brünger, A. T. (1989) *Acta Crystallogr. A45*, 50–61.

Brünger, A. T. (1990) *Acta Crystallogr. A46*, 46–57.

Carreras, C. W., Climie, S. C., & Santi, D. V. (1992) *Biochemistry 31*, 6038–6044.

Climie, S., Ruiz-Perez, L., Gonzalez-Pacanowska, D., Prapunwattana, P., Cho, S.-W., Stroud, R., & Santi, D. V. (1990) *J. Biol. Chem. 265*, 18776–18779.

Climie, S. C., Carreras, C. W., & Santi, D. V. (1992) *Biochemistry 31*, 6032–6038.

Da, Y.-Z., Ito, K., & Fujiwara, H. (1992) *J. Med. Chem. 35*, 3382–3387.

Daron, H. H., & Aull, J. L. (1978) *J. Biol. Chem. 253*, 940–945.

Dev, I. K., Yates, B. B., Leong, J., & Dallas, W. S. (1988) *Proc. Natl. Acad. Sci. U.S.A. 85*, 1472–1476.

Devereux, J., Haeberli, P., & Smithies, O. (1984) *Nucleic Acids Res. 12*, 387–395.

Dill, K. A., Alonso, D. O. V., & Hutchison, K. (1989) *Biochemistry 28*, 5439–5449.

Fauman, E. B. (1993) Ph.D. Thesis, University of California, San Francisco.

Finer-Moore, J. S., Montfort, W. R., & Stroud, R. M. (1990) *Biochemistry 29*, 6977–6986.

Finer-Moore, J., Fauman, E. B., Foster, P. G., Perry, K. M., Santi, D. V., & Stroud, R. M. (1993) *J. Mol. Biol. 232*, 1101–1116.

Fox, G. C., & Holmes, K. C. (1966) *Acta Crystallogr. 20*, 886–891.

French, S., & Wilson, K. (1978) *Acta Crystallogr. A34*, 517.

Galivan, J. H., Maley, G. F., & Maley, F. (1976) *Biochemistry 15*, 356–362.

Galivan, J., Maley, F., & Baugh, C. M. (1977) *Arch. Biochem. Biophys. 184*, 346–354.

Hansch, C. H., & Leo, A. (1979) in *Substituent Constants for Correlation Analysis in Chemistry and Biology*, Wiley, New York.

Hardy, L. W., Finer-Moore, J. S., Montfort, W. R., Jones, M. O., Santi, D. V., & Stroud, R. M. (1987) *Science 235*, 448–455.

Hendrickson, W. A., & Konnert, J. H. (1981) in *Biomolecular Structure, Conformation, Function and Evolution* (Srinivasan, R., Subramanian, E., & Yathindra, N., Eds.) Vol. I, pp 43–57, Pergamon Press, New York.

Jones, T. A. (1985) *Methods Enzymol. 115*, 157–171.

Kabsch, W. (1978) *Acta Crystallogr. A34*, 827–828.

Kamb, A., Finer-Moore, J., Calvert, A. H., & Stroud, R. M. (1992a) *Biochemistry 31*, 9883–9890.

Kamb, A., Finer-Moore, J. S., & Stroud, R. M. (1992b) *Biochemistry 31*, 12876–12884.

Kraulis, P. J. (1991) *J. Appl. Crystallogr. 24*, 946–950.

Kunitani, M. G., & Santi, D. V. (1980) *Biochemistry 19*, 1271–1275.

Lamm, N., Tomaschewski, J., & Ruger, W. (1987) *Nucleic Acids Res. 15*, 3920.

Lorenson, M. Y., Maley, G. F., & Maley, F. (1967) *J. Biol. Chem. 242*, 3332–3344.

Lundqvist, T., & Schneider, G. (1991) *Biochemistry 30*, 904–908.

Maley, G. F., & Maley, F. (1988) *J. Biol. Chem. 263*, 7620–7627.

Maley, G. F., & Maley, F. (1989) *Adv. Enzyme Regul. 29*, 181–187.

Matthews, D. A., Appelt, K., Oatley, S. J., & Xuong, N. H. (1990a) *J. Mol. Biol. 214*, 923–936.

Matthews, D. A., Villafranca, J. E., Janson, C. A., Smith, W. W., Welsh, K., & Freer, S. (1990b) *J. Mol. Biol. 214*, 937–948.

Montfort, W. R., Perry, K. M., Fauman, E. B., Finer-Moore, J. S., Maley, G. F., Hardy, L., Maley, F., & Stroud, R. M. (1990a) *Biochemistry 29*, 6964–6977.

Montfort, W. R., Fauman, E. B., Perry, K. M., & Stroud, R. M. (1990b) in *Current Research in Protein Chemistry: Tech-*

niques, Structure and Function (Villafranca, J. J., Ed.) pp 367–382, Harcourt Brace Jovanovich, San Diego.
Otwinowski, Z. (1986) in *DENZO manual*, University of Chicago, Chicago, IL.
Perry, K. M., Fauman, E. B., Finer-Moore, J. S., Montfort, W. R., Maley, G. F., Maley, F., & Stroud, R. M. (1990) *Proteins 8*, 315–333.
Perry, K. M., Carreras, C. W., Chang, L. C., Santi, D. V., & Stroud, R. M. (1993) *Biochemistry 32*, 7116–7125.
Pogolotti, A. L. J., & Santi, D. V. (1977) *Bioorg. Chem. 1*, 277–311.
Ponder, J. W., & Richards, F. M. (1987) *J. Mol. Biol. 193*, 775–791.
Quiocho, F. A., Wilson, D. K., & Vyas, N. K. (1989) *Nature 340*, 404–407.
Rashin, A. A., Iofin, M., & Honig, B. (1986) *Biochemistry 25*, 3619–3625.
Ross, P., O'Gara, F., & Condon, S. (1990) *Appl. Environ. Microbiol. 56*, 2156–2163.
Santi, D. V., & Danenberg, P. V. (1984) in *Folates and Pterins: Vol. 1, Chemistry and Biochemistry of Folates* (Blakely, R. L., & Benkovic, S. J., Eds.) pp 345–399, John Wiley & Sons, New York.
Schiffer, C. A., Davisson, V. J., Santi, D. V., & Stroud, R. M. (1991) *J. Mol. Biol. 219*, 161–163.
Shoichet, B. K., Stroud, R. M., Santi, D. V., Kuntz, I. D., & Perry, K. M. (1993) *Science 259*, 1445–1450.
Stroud, R. M., & Finer-Moore, J. S. (1993) *FASEB J. 7*, 671–677.
Taylor, J. W., Ott, J., & Ekstein, F. (1985) *Nucleic Acids Res. 13*, 8765–8785.
Thylen, C. (1988) *J. Bacteriol. 170*, 1994–1998.
Vriend, G., Berendsen, H. J. C., van der Zee, J. R., van den Burg, B., Venema, G., & Eijsink, V. G. H. (1991) *Protein Eng. 4*, 941–945.
Wilhelm, K., & Ruger, W. (1992) *Virology 189*, 640–646.
Wilson, A. J. C. (1949) *Acta Crystallogr. 2*, 318–321.